Electronic Supplementary Information (ESI)

Aptamer-functionalized Exosomes from Bone Marrow Stromal Cells Target Bone to Promote Bone Regeneration

Zhong-Wei Luo[#], Fu-Xing-Zi Li[#], Yi-Wei Liu, Shan-Shan Rao, Hao Yin, Jie Huang, Chun-Yuan Chen, Yin Hu, Yan Zhang, Yi-Juan Tan, Ling-Qing Yuan, Tuan-Hui Chen, Hao-Ming Liu, Jia Cao, Zheng-Zhao Liu, Zhen-Xing Wang and Hui Xie**

Contents

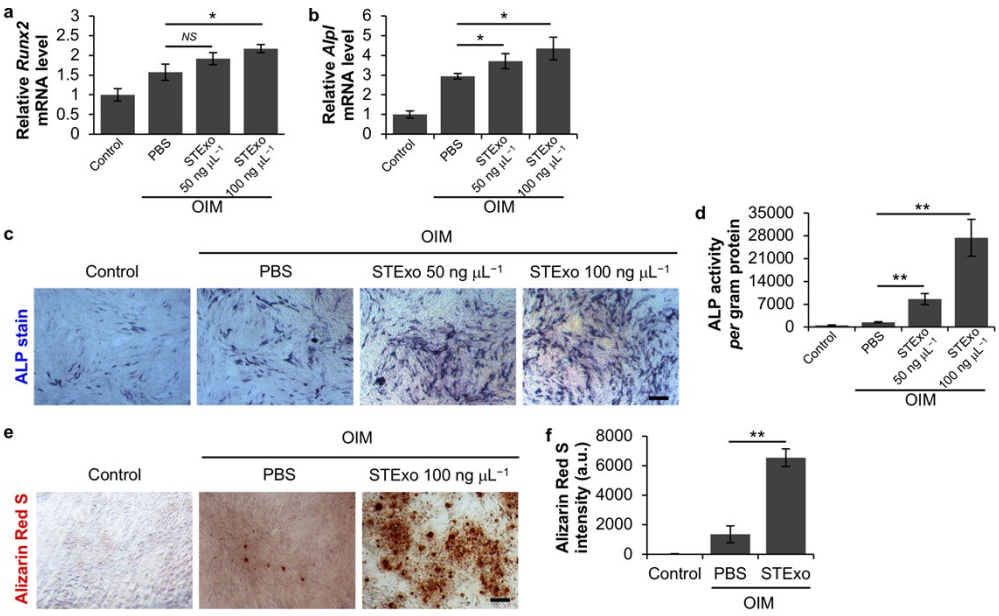

Figure S1. STExo enhanced osteoblastic differentiation of bone marrow mesenchymal stem cells (BMSCs) and bone marrow stromal cells (STs). (a,b) qRT-PCR analysis of *Runx2* (a) and *Alpl* (b) expression levels relative to *Gapdh* in BMSCs. $n = 3$ *per* group. (c,d) Representative images of ALP staining showing strong blue color in BMSCs (c) and quantitative analysis of the ALP activity normalized to cellular protein amount (d). Scale bar: 100 μm. $n = 3$ *per* group. (e,f) Representative images of Alizarin Red S staining showing red mineralized nodules in STs (e) and quantitative analysis of the mineralization intensity (f). Scale bar: 100 μm. $n = 3$ *per* group. OIM: osteogenesis induction medium. * $P < 0.05$, ** $P < 0.01$, *NS,* not significant.

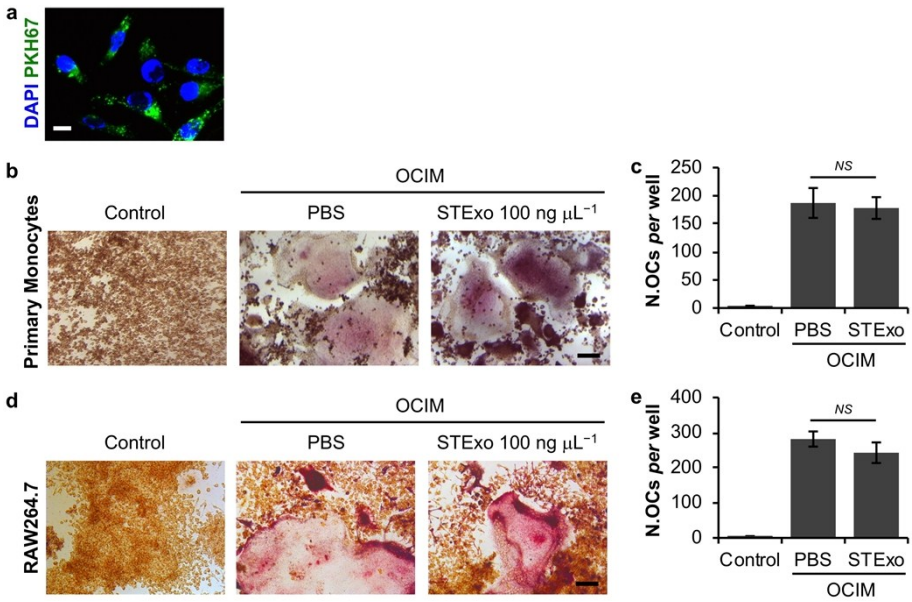

Figure S2. STExo didn't affect the osteoclastic differentiation of the mouse primary monocytes/macrophages and cell line RAW264.7. (a) Representative fluorescent microscopic images of green florescent dye PKH67-labeled STExo (STExo-PKH67) internalized by

RAW264.7 cells. The cell nucleus was stained with DAPI (blue). Scale bar: 10 μm. (b-e) Representative images of Trap staining showing purple color in osteoclasts (b,d) and quantitative analysis of the osteoclast numbers (c,e). OCIM: osteoclastogenesis induction medium. Scale bar: 100 μm. $n = 3$ *per* group. *NS,* not significant.

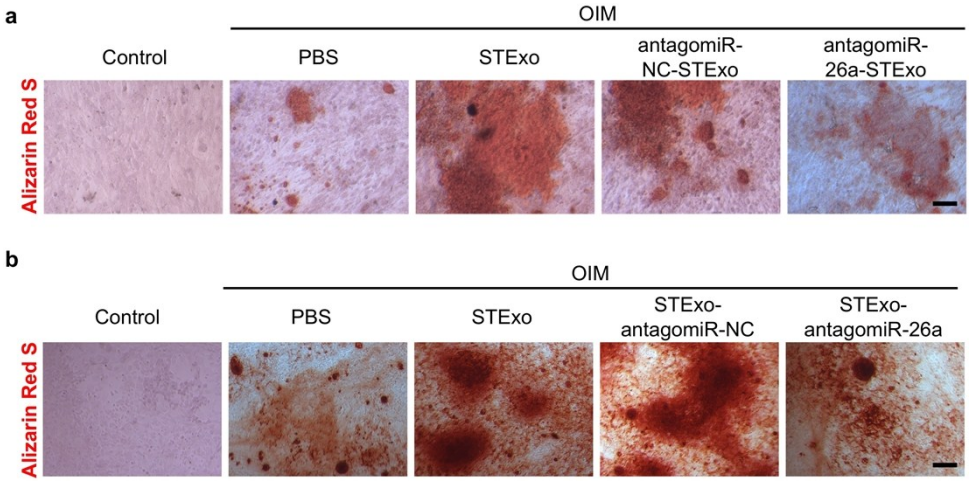

Figure S3. Exosomal miR-26a is the key osteogenesis stimulator in STExo. (a,b) Representative images of Alizarin Red S staining showing red mineralized nodules in BMSCs under the indicated different treatments. OIM: osteoblastic induction medium. Scale bar: 100 μm. $n = 3$ *per* group. * $P < 0.05$, ** $P < 0.01$.

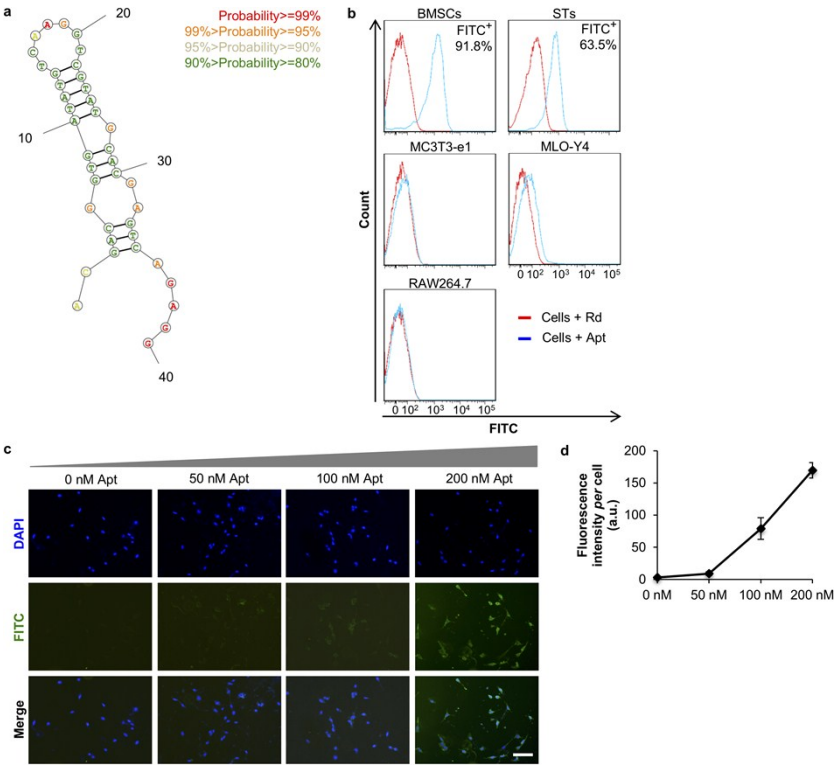

Figure S4. The specific aptamers targeting BMSCs. (a) The aptamer structure was predicted by RNAStrcuture Website. The multicolor of bases indicated the structure probability. (b) The flow cytometry assay to monitor the aptamer specific targeting with BMSCs, STs, MC3T3-e1, MLO-Y4 and RAW264.7 cells. (c,d) Representative images of fluorescence of increased concentrations of FITC-labeled aptamers (green) from 0 to 200 nM in BMSCs (c) and quantitative analysis of the fluorescence intensity *per* cell (d). The nucleus was stained with DAPI (blue). Scale bar: 100 μm. $n = 3$ *per* group.

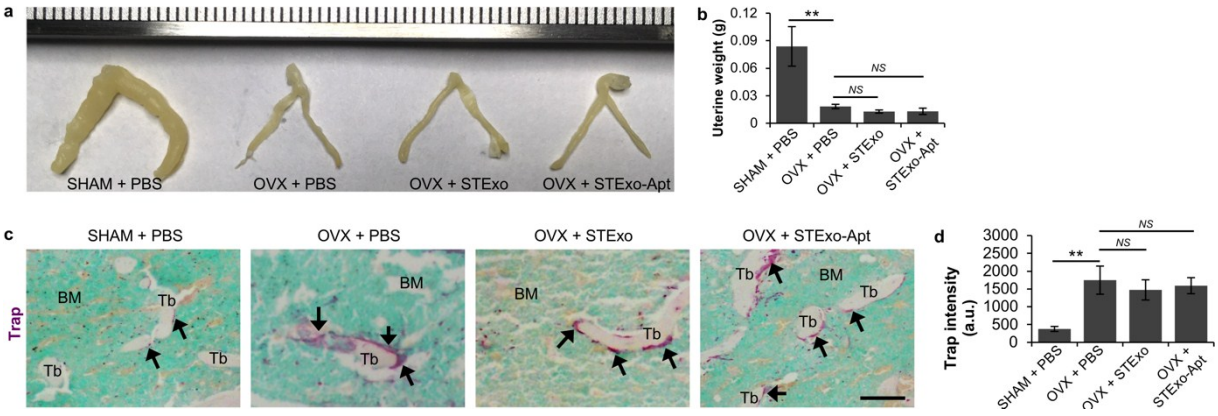

Figure S5. STExo-Apt rescued bone loss in OVX mice model. (a,b) Representative images of dissect uterus after two months treatment (a) and quantitative analysis of uterus weight (b). (c) Representative images of Trap staining of femora. The black arrows indicate the positive staining areas. Tb: trabecular bone; BM: bone marrow. Scale bar: 100 μm. (d) Quantitative analysis of the intensity for the positive staining areas in (c). $n = 4$ *per* group. ** $P < 0.01$, *NS,* not significant.